Bearing Capacity of Piles and Pile Groups

Le Pouvoir Portant des Pieux et des Groupes de Pieux

by Á. KÉZDI, Budapest, XI., Budafoki-u. 4, Hungary

Summary

The author deduces a semi-empirical law relating skin friction to strain for the case of piles embedded in sand. This new law enables the loading test diagram for piles to be constructed. Piles supported exclusively by skin friction and piles with point support are dealt with, as simple cases; then the composite problem is solved. The general case exhibits the nature of local shear failures; there is no sharp break at failure, the loading diagram continues to slope.

The theoretical results are supported by model tests carried out in the laboratory and in the field. Field test results are used to determine the constants of the equations.

The ultimate load of pile groups is determined by large model tests in the field. The ultimate load of pile rows and of four piles placed at the corners of a square is surprisingly greater than four times the ultimate load of a single pile, and the settlement is considerably smaller.

Sommaire

L'auteur déduit une loi de cisaillement entre les contraintes et les déplacements pour le cas des pieux dans le sable. La nouvelle loi permet de construire le diagramme des essais de pieux; la solution du problème des pieux flottants, des pieux travaillant à la pointe, est décrite, puis celle du cas des pieux mixtes. Ce cas général montre la nature de la rupture locale de cisaillement; il n'y a pas de discontinuité à la rupture; le diagramme est continu.

Les essais sur modèle réduit confirment les résultats théoriques. Les constantes des équations sont déterminées à l'aide d'un essai sur chantier.

La force portante du groupe de pieux fut déterminée par des essais sur grands modèles. La force de rupture de quatre pieux battus et rangés sur une ligne, ou en carré est plus grande que quatrefois la force portante d'un seul pieu, ce qui est très surprenant, l'enfoncement étant considérablement plus petit.

Research on piles has already shown in detail that the so-called dynamic pile driving formulae and the static relationships based on the earth pressure theories are not suitable for determining the bearing capacity. The determination of the safe load on the basis of loading diagrams taken in the course of a load test also presents difficulties, either because the value of the ultimate load could not be reached or because general shear failure does not occur: the loading diagram does not become vertical but continues to slope; there is no failure point. A further problem arises with the bearing capacity of pile groups. Theoretical investigations have so far covered individual piles; actual observations, however, have shown that the settlement of a group of piles can hardly be correlated with that of the individual pile. Deformations require more consideration in the investigation of the bearing capacity of piles; pile foundations should be designed on the basis of allowable settlement.

This paper aims at contributing to the elucidation of the controversial problems in this field by the theoretical determination of the loading diagram of individual piles and by presenting the results of systematic model tests.

Theoretical Determination of the Loading Diagram of an Individual Pile

(1) To determine the inter-relation between load and settlement a new law of shear is introduced. This law was deduced from measurements of the angle of shearing resistance between granular materials and other construction materials in a shear test apparatus of 30 × 30 cm² surface and with strain control. A characteristic experimental result is shown in Fig. 1. For the ratio of stresses τ and σ pertaining to full shear the Coulomb line is obtained; on the other hand, if the value of the shearing stresses associated with a certain horizontal displacement ρ is plotted as a function of the corresponding normal stresses, similar straight lines are obtained. The amount of displacement necessary for the development of full friction varies within close limits so that the sought relation can be approached for cohesionless soils by the following law of shear:

$$\tau = \sigma \tan \phi \left[1 - \exp\left(-k \frac{\rho}{\rho_0 - \rho}\right)\right] \qquad \ldots . (1)$$

In the formula τ is the shear stress required for producing a displacement ρ at normal stress σ; ϕ is the angle of full shearing resistance; ρ_0 is the shear displacement necessary for the development of full friction; k is a constant depending on the kind and the compactness of the soil.

For example, Fig. 2 presents plots taken during a shear test of a sandy gravel on a concrete surface and the values are

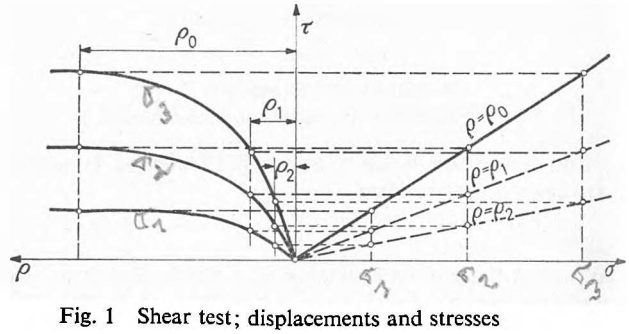

Fig. 1 Shear test; displacements and stresses
Essai de cisaillement; et contraintes déplacements

computed by equation 1. Similar good agreement was found in numerous cases.

Equation 1 satisfies the boundary conditions: if $\sigma = 0$, $\tau = 0$; if $\rho = 0$, $\tau = 0$; if $\rho = \rho_0$, $\tau = \sigma \tan \phi$ and $\partial\tau/\partial\rho = 0$. The constant k is determined by the slope of the tangent to the curve $\tau = f(\rho)$ at the origin:

$$\left(\frac{\partial \tau}{\partial \rho}\right)_{\rho=0} = \frac{k}{\rho_0}; \quad k = \rho_0 \tan \alpha_0 \qquad \ldots . (2)$$

(2) Let the loading diagram of the pile be investigated on the basis of this law of shear. The pile will first be regarded as a rigid, weight-less cylindrical column embedded into a homogeneous granular material; there is no point resistance and the pile is floating. Under the effect of a given penetration ρ, resistances to shear develop; their sum is equal to the force P acting on the pile. In the case of bored piles the earth pressure

at rest is acting as a normal stress on the peripheral surface ($\sigma = K_0 z\gamma$), hence:

$$P = \int_{z=0}^{l} \tau K dz = \int_0^l K K_0 \gamma z \tan\phi \left[1 - \exp\left(-k\frac{\rho}{\rho_0 - \rho}\right)\right] dz$$

(K = circumference of pile)

$$P = K_0 \gamma K \tan\phi \frac{l^2}{z}\left[1 - \exp\left(-k\frac{\rho}{\rho_0 - \rho}\right)\right] \quad \ldots . \quad (3)$$

Fig. 3 presents a curve taken in the course of a model test; the point resistance being eliminated.

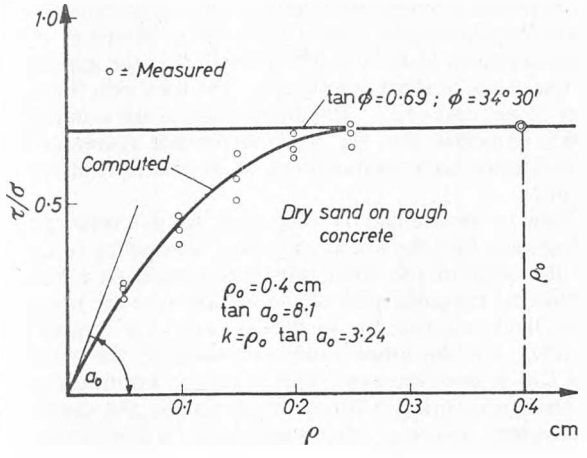

Fig. 2 Example of shear test
Exemple d'essai de cisaillement

The load applied to the pile at the head is gradually transmitted to the surroundings through skin friction; at depth z in the profile it is:

$$P_z = C\left[1 - \exp\left(-k\frac{\rho}{\rho_0 - \rho}\right)\right](l^2 - z^2) \quad \ldots . \quad (4)$$

where $C = \frac{1}{2}K_0\gamma \tan\phi K$.

A numerical example is shown in Fig. 4; for different displacements ρ the curves described by equation 4, the distribution of the skin friction, and the loading diagram of the pile are presented.

(3) The other limiting case is the point-bearing pile with a fixed pile point, Fig. 5. If ρ is the displacement of the pile at depth z, then the vertical strain is $d\rho/dz = P/EA$, where E is Young's modulus for the pile and A is its area of cross-section, therefore

$$P = EA\frac{d\rho}{dz}; \quad \frac{dP}{dz} = EA\frac{d^2\rho}{dz^2}$$

If the shear stress associated with a displacement ρ is $\tau(\rho)$, then

$$dP = \tau(\rho)K dz$$

$$\frac{dP}{dz} = \tau(\rho)K$$

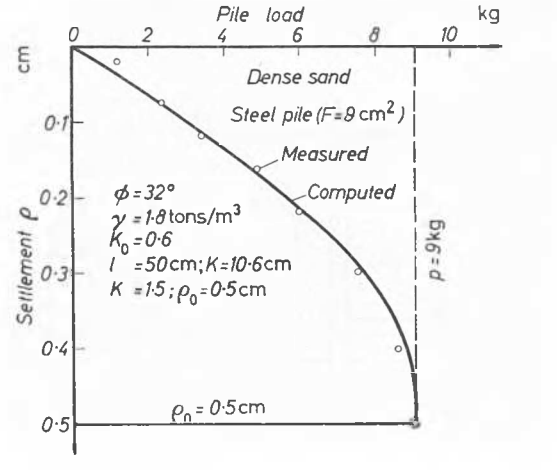

Fig. 3 Settlement of pile with free end; model test result
Enfoncement de pieu avec pointe libre: essais sur modèle réduit

and finally

$$\frac{d^2\rho}{dz^2} = \frac{K}{EA}\tau(\rho) \quad \ldots . \quad (5)$$

In this case deformations result only from the elastic compression of the material of the pile: because these are small it may be assumed, with good approximation, that the relation between the skin friction and the displacement is linear. That is $\tau = \sigma \tan\phi(\rho/\rho_0)$. Then, again in the case of a bored pile,

$$\frac{d^2\rho}{dz^2} = \frac{K}{EA}K_0\gamma \tan\phi \frac{1}{\rho_0}\rho z$$

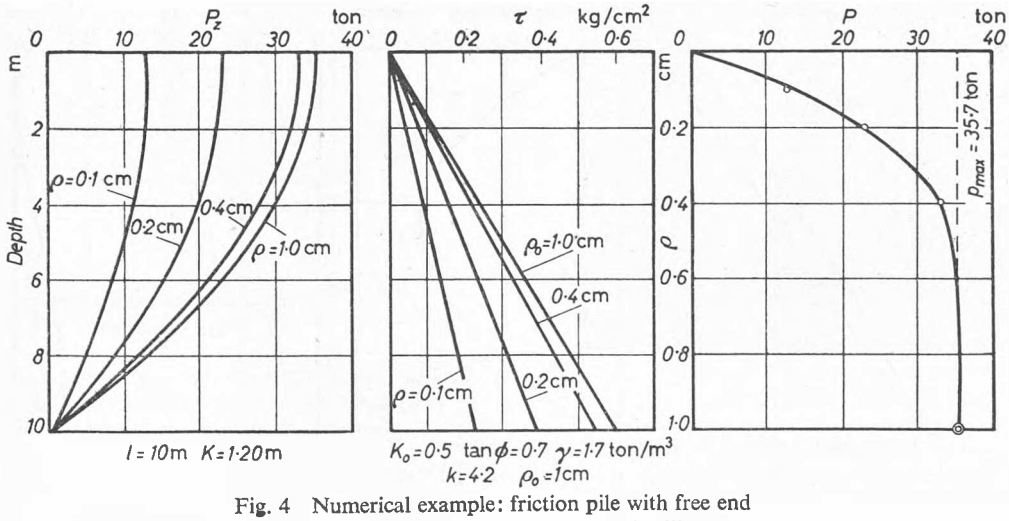

Fig. 4 Numerical example: friction pile with free end
Exemple numérique, pieu avec point libre

Let

$$\frac{K}{EA}K_0\gamma \tan\phi\frac{1}{\rho_0} = \alpha$$

$$\frac{d^2\rho}{dz^2} - \alpha\rho z = 0 \qquad \ldots\ (6)$$

The general solution of the differential equation 6 is:

$$\rho = A_0\left(1 + \frac{\alpha}{2.3}z^3 + \frac{\alpha^2}{2.3.5.6}z^6 + \frac{\alpha^3}{2.3.5.6.8.9}z^9 + \ldots\right) + A_1\left(z + \frac{\alpha}{3.4}z^4 + \frac{\alpha^2}{3.4.6.7}z^7 + \frac{\alpha^3}{3.4.6.7.9.10}z^{10} + \ldots\right) \qquad \ldots\ (7)$$

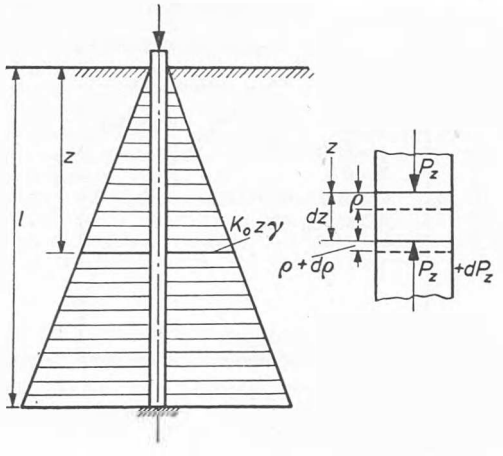

Fig. 5 Stresses acting on the periphery of a pile; fixed pile point condition
Contraintes latérales sur la surface de pieu; la pointe étant fixé

The boundary conditions are:

$$\text{(a)}\ z = 0,\quad \frac{d\rho}{dz} = \frac{P}{EA} = \epsilon_0$$

$$\text{(b)}\ z = l,\quad \rho = 0 \qquad \ldots\ (8)$$

That is

$A_1 = \epsilon_0$ the vertical displacement of the head of the embedded pile;

and

$$A_0 = -\epsilon_0 l\frac{1 + \frac{\alpha}{3.4}l^3 + \frac{\alpha^2}{3.4.6.7}l^6 + \ldots}{1 + \frac{\alpha}{2.3}l^3 + \frac{\alpha^2}{2.3.5.6}l^6 + \ldots}$$

After the determination of the constants the vertical displacement of the different points of the pile can be computed from equation 7; and from these displacements the shearing stresses. Finally the proportion of the force P acting on the pile head, which is transmitted to the fixed pile point, can be calculated.

Fig. 6 shows a numerical example: the displacements of a $l = 10$ m long timber pile, loaded at the pile head with $P = 40$ t. The displacements of the pile are so small that the application of the linear law of shear is justified. The total skin friction is scarcely 15 per cent of P. The distribution of the skin friction follows a parabolic law, the force in the pile decreases with depth as friction becomes mobilized by the elastic displacement of the pile.

(4) Now let us examine the case when the pile penetrates as a rigid column into the soil at its point. According to GEUZE (1955) the value of the point resistance cannot be calculated from physical characteristics of the soil because the necessary physical and mechanical quantities are not measurable practically. On the other hand, according to the empirical data of KEVERLING-BUISMAN (1955), it may be assumed that the point resistance varies in direct proportion to the depth and pile diameter. However, that supposition is applicable only if we consider a sounding rod surrounded with a pipe and loaded at its point, with the skin friction eliminated. In the case of an embedded pile, the load transmitted through the periphery increases the vertical stress acting in the plane of pile point and hence the point resistance is in direct proportion to that stress and not to the depth. Let us suppose as an approximation that the force transmitted through the skin friction causes a uniformly distributed load on a circle in the plane of the pile point having a radius $nr (n \approx 5, B = 2r)$. Then, equilibrium requires,

$$P = P_P + P_S = a\rho B\left(l\gamma + \frac{4P_S}{n^2B^2\pi}\right) + P_S \qquad \ldots\ (9)$$

where

$$P_S = K_0 B\pi\frac{l^2}{2}\tan\phi\gamma\left[1 - \exp\left(-k\frac{\rho}{\rho_0 - \rho}\right)\right]$$

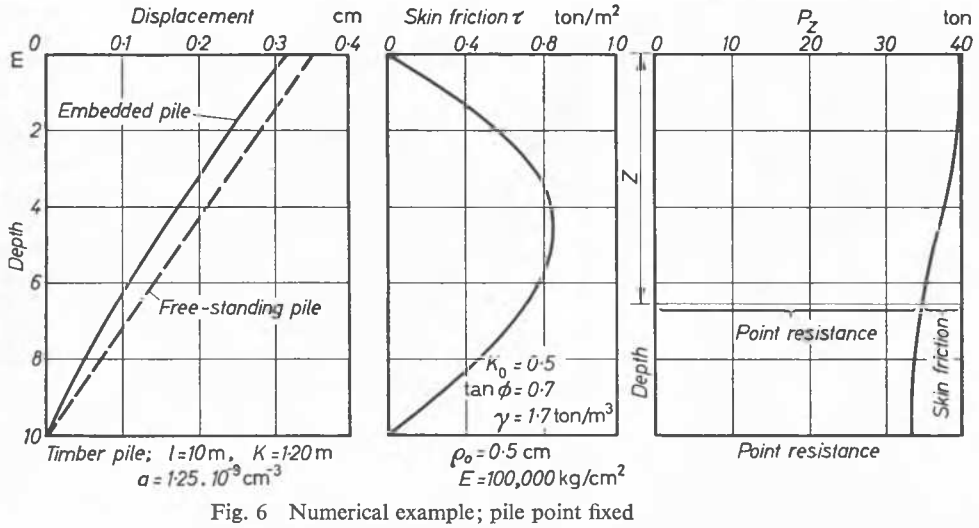

Fig. 6 Numerical example; pile point fixed
Exemple numérique, la pointe du pieu est fixé

The load-displacement curve of the pile can be drawn from equation 9; Fig. 7 shows an example. The diagram, as in the case of actual test diagrams, continues to slope and there is no general shear failure. The relation shows that point resistance and skin friction depend on each other; both are functions of displacement. When $\rho \geqslant \rho_0$ the skin friction is fully mobilized

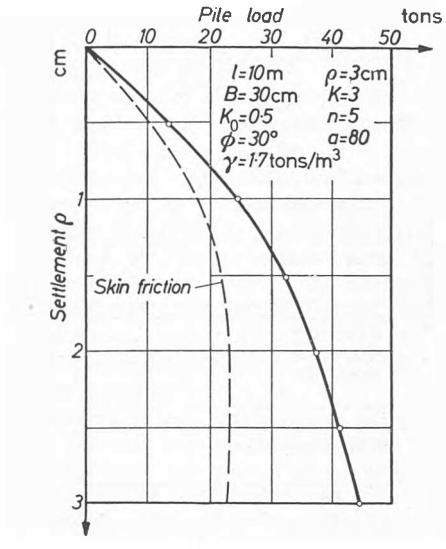

Fig. 7 Load–settlement curve of a pile with both point resistance and skin friction
Enfoncement d'un pieu avec résistance à la pointe et frottement latérale

and cannot increase; point resistance is then proportional to penetration. The factor of proportionality a, is a pure number, a function of the angle of internal friction and a modulus of elasticity. The establishment of a strict mathematical relationship seems impossible for the time being. It must be emphasized that equation 9 applies only to the case where

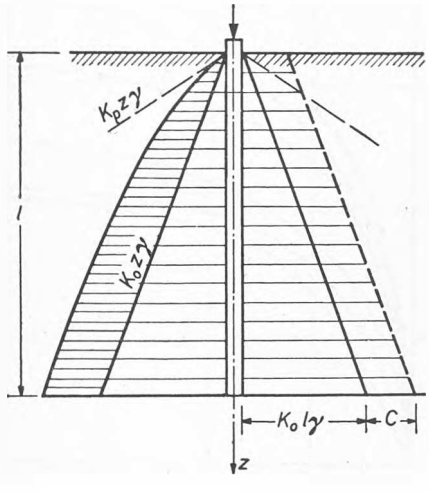

Fig. 8 Stresses acting on the periphery of a driven pile
Contraintes latérales sur la surface d'un pieu battu

cohesionless soil surrounds the pile. Piles driven through clay soils with the pile points bearing in sand or gravel call for investigation of the three-dimensional failure beneath pile points; in this case the skin friction is of less importance (see case treated in sub-section (3) and proportionality between point resistance and displacement cannot be assumed.

(5) Around driven piles substantial compaction of the soil takes place, the amount being equal to the volume of the pile. In consequence it is no longer the static pressure that acts on the surface of the pile, but a greater one, depending on the diameter of the pile and on the initial compactness of the sand.

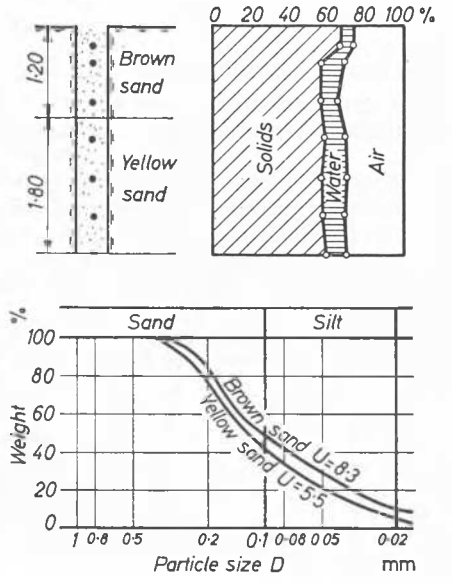

Fig. 9 Physical data of the soil at the test pile site
Caractéristiques physiques du sol du chantier des essais

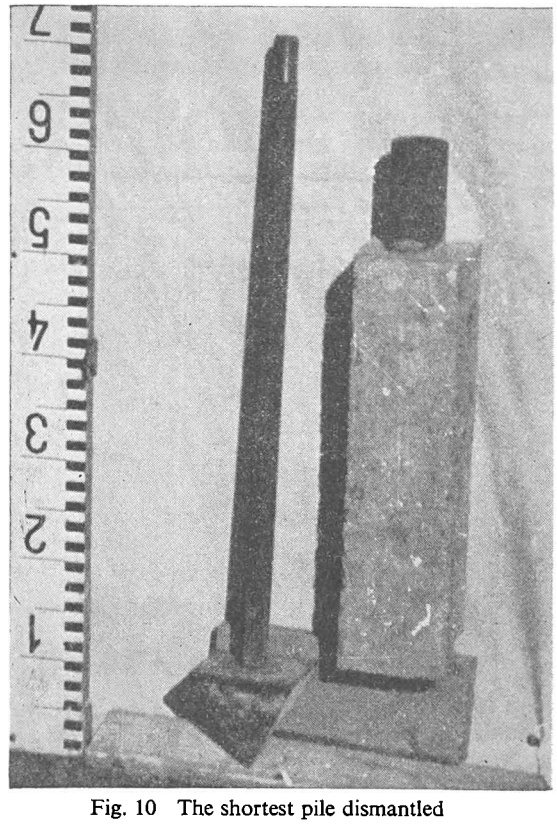

Fig. 10 The shortest pile dismantled
Le pieu le plus court démonté

The distribution of the normal stress will be according to Fig. 8; near to the surface the passive stress state will be approached, and in the deeper layers an approximately constant normal stress will be added to the static pressure. If the radius of the

cylinder, within which displacements take place in consequence of driving, is denoted by R (this value being proportional to the radius r of the pile) the volume strain is $e = r^2/R^2 = 1/\beta^2$, from which the pressure acting on the surface of the pile is already calculable by the Theory of Elasticity or by making use of the findings of STEINFELD (1953).

Ultimate Load Capacity of an Individual Pile

Large model tests carried out in the field were used to investigate the ultimate load capacity. Concrete piles of different lengths (l = 0·40; 0·80; 1·20; 1·60 and 2·0 m) of 10 × 10 cm² cross-sectional area were driven into homogeneous fine grained sand the physical data of which is given in Fig. 9. The pile points could be loaded separately. The shortest pile is shown dismantled in Fig. 10.

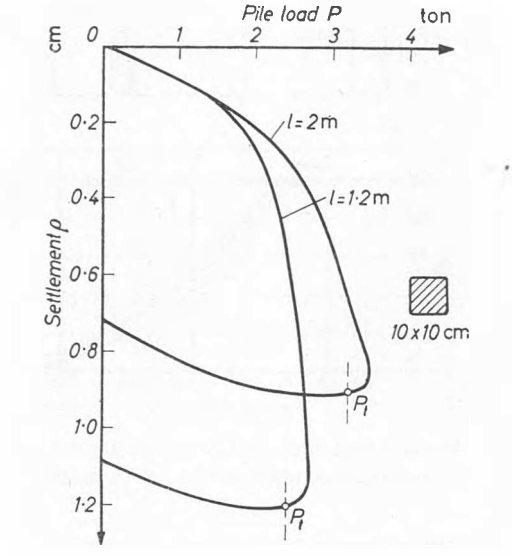

Fig. 11 Load-settlement curve of single piles
Diagramme de charge des pieux individuels

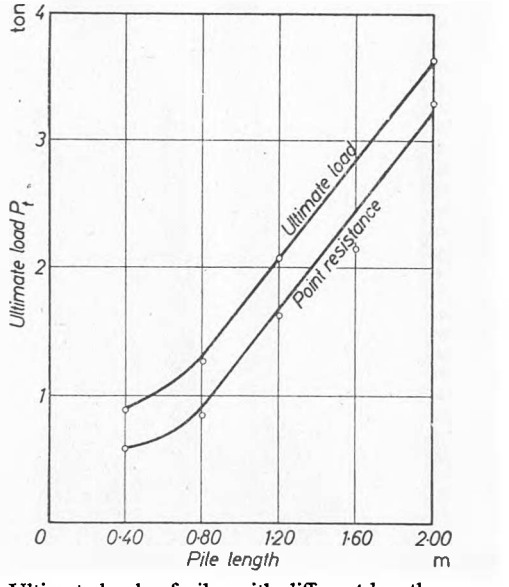

Fig. 12 Ultimate loads of piles with different length
Force de rupture des pieux avec des longueurs différentes

Two characteristic loading diagrams are shown in Fig. 11. The shape of the curve corresponds to the case given under subsection 4 in the previous section; general shear failure did not take place. On unloading the settlement increased a little, and subsequently elastic rebound occurred. The force corresponding to maximum penetration was regarded as the ultimate load. The constants in the theoretical equation of the loading curve were computed from one of the experimental curves; and hence the loading diagrams pertaining to the other pile lengths were calculated. For piles of 1·20 and 1·60 m length the computed and measured data showed good agreement. In the case of the shorter piles the assumptions do not hold; when $l < 8\ B$ no real pile effect occurred. In practical cases a loading test is the best way of determining the constants.

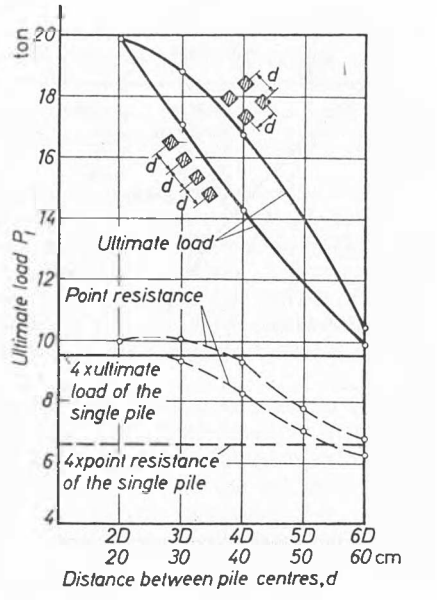

Fig. 13 Ultimate loads of pile groups
Force de rupture des groupes de pieux

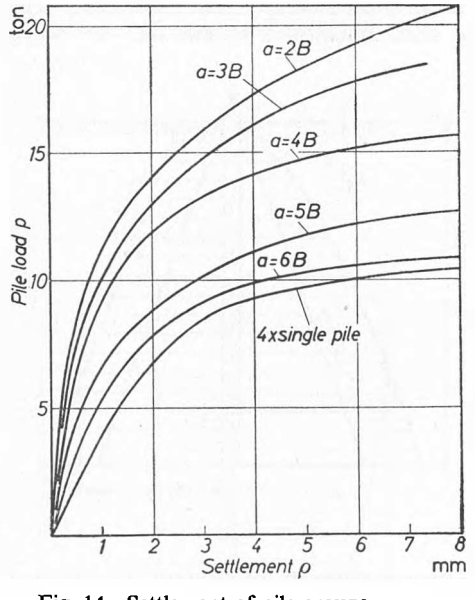

Fig. 14 Settlement of pile groups
Enfoncement des groupes de pieux

The ultimate load interpreted according to the foregoing is shown in Fig. 12 as a function of the pile length. Measured values show here the same regularity as laboratory model tests (KEZDI, 1955); beyond a critical depth, which is about 8 times

the pile diameter; the relationship can be represented by a straight line.

Bearing Capacity of Pile Groups

There are few experimental data or little theoretical research on the bearing capacity of pile groups in the literature. The qualitative statement generally accepted is that in the case of a point-bearing pile the bearing capacity of the pile group is n times that of the individual pile, while in the case of friction piles it is less than that value.

To further the solution of the problem field tests in addition to laboratory experiments were extended to the investigation of pile groups. Four piles ($l = 2{\cdot}0$ m; $A = 10 \times 10$ cm^2) were driven in a row, and at the corners of a square, and loading diagrams were taken at different pile spacings. The relation between ultimate load of the group and the pile centres is shown in Fig. 13; the horizontal line denotes the fourfold bearing capacity of the single pile. Both in the case of piles driven in a row and at the corners of a square, the bearing capacity of the group is substantially higher than that; only at $d = 6B$ does the group capacity reduce to that of the single pile. At $d = 2B$ the increase is more than 100 per cent.

The explanation is that in the case of piles driven closely to one another the soil core enclosed between the piles is substantially compacted, and moves along with the piles and a larger loaded surface develops in the plane of pile points. Therefore the law established for sand is valid: the ultimate load increases with the width of the loaded area. Superposition of piles is therefore favourable from the point of view of ultimate bearing capacity; in the plane of the pile point the loading of the adjacent piles increases the vertical stresses and failure sideways is less likely to occur. The group action discontinues for piles driven at $d = 6B$ centres.

Fig. 14 shows the magnitude of loads causing given pile settlements. The less the distance between pile centres, the smaller will be the settlement under a given load; at $d = 6B$ between centres the loading diagram approaches the line giving the fourfold loading of the individual pile as a function of its settlement. The groups thus behaved very favourably from the point of view of settlement, most probably due to soil compaction caused by the driving.

The above facts, of course, cover only the case when there is no more compressible layer beneath pile points. In that case, the vertical stresses transmitted at the level of a close group of pile points will penetrate to much greater depths than below a single pile and cause greater settlement.

The author wishes to express his sincere thanks to Research Engineer H. Herzog for carrying out the experiments and supervizing the field tests.

References

GEUZE, E. C. W. A. (1955). Fortschritte unserer Kenntnisse über die Tragfähigkeit von Pfahlspitzen. *Vorträge der Baugrundtagung 1954 in Stuttgart*. Hamburg

KÉZDI, Á. (1955). Über die Tragfähigkeit und Setzung von Pfahlgründungen. *Gedenkbuch für Professor J. Jáky*. Budapest

STEINFELD, K. (1953). Ueber den räumlichen Erdwiderstand. *Mitteilungen der Hannoverschen Versuchsanstalt für Grundbau und Wasserbau*, Heft 3

KEVERLING-BUISMAN, A. S. (1955). *Vorträge der Baugrundtagung 1954 in Stuttgart*. Hamburg